Chapter 1

Application of an Electric Field to Low-Frequency Oscillation Control in Hall Thrusters

Liqiu Wei, Yongjie Ding and Daren Yu

Additional information is available at the end of the chapter

http://dx.doi.org/10.5772/intechopen.71009

Abstract

In order to satisfy the national demands for developing a long-life satellite platform, lunar exploration, and deep-space exploitation, Hall thrusters are now considered the preferred candidate for spacecraft propulsion. A Hall thruster is a type of electric propulsion with an annular structure, in which a propellant, usually xenon, is ionized and then accelerated by electrostatic force to create a propulsive thrust. Low-frequency discharge current oscillations, also called breathing mode oscillations in some references, are among the major research topics of Hall thrusters. Low-frequency oscillations in the range of 10–100 kHz might affect the reliability of power processing unit and reduce the efficiency and specific impulse of Hall thrusters. The control of low-frequency oscillations is an essential challenge in the space application of Hall thrusters. It is proved that the electric field is a highly important influence factor for low-frequency oscillations; therefore, application of a dynamic electric field is a practical way to control low-frequency oscillation.

Keywords: electric field, low-frequency oscillation, control, filter unit, Hall thruster

1. Introduction

In order to adapt the technology requirements of surveying deep space and conducting interplanetary travel, it is an inexorable trend in the development of spacecraft propulsion systems that electric propulsion will take the place of chemical propulsion. A Hall thruster is a type of electric propulsion with an annular structure, in which a propellant, usually xenon, is ionized and then accelerated by electrostatic force to create a propulsive thrust. The typical configuration is shown in **Figure 1**. A mostly transverse magnetic flux is produced by the magnetic circuit and magnetic coils in the discharge channel, with a maximum radial intensity near the channel exit. The discharge voltage is applied between the anode and an external hollow cathode. The propellant, usually Xenon, is injected through the gas distributor. The

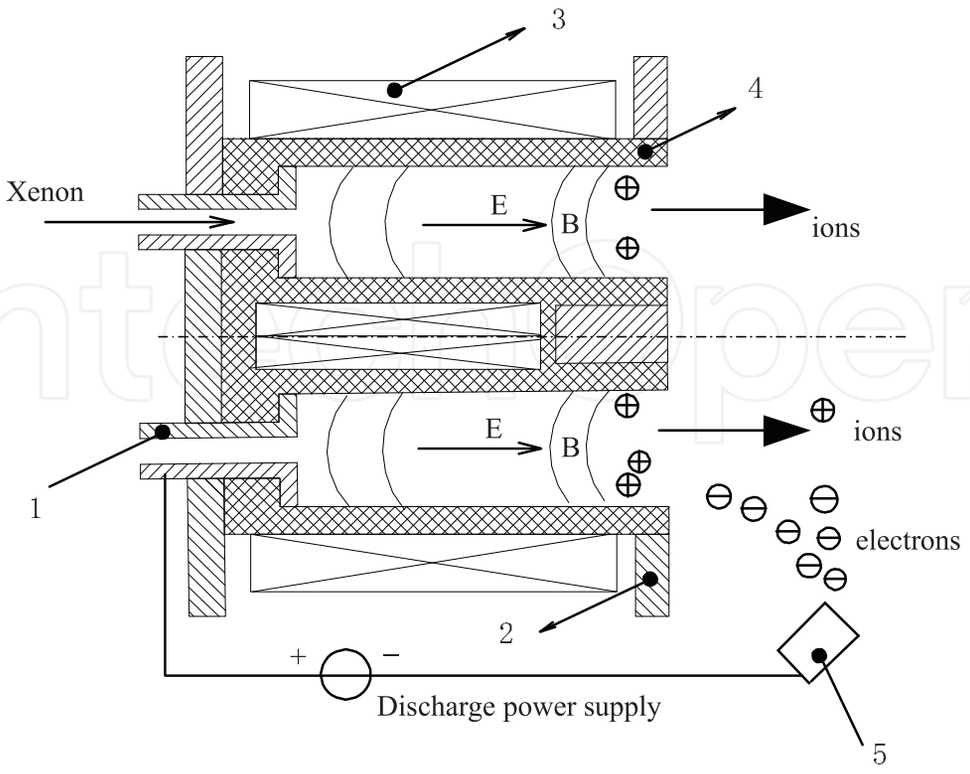

Figure 1. Schematic diagram of a Hall thruster: (1) anode, (2) magnetic pole, (3) magnetic coils, (4) accelerating channel, and (5) cathode.

magnetic field limits the axial mobility of electrons and then causes a localized voltage drop of the order of the anode-cathode discharge voltage. Electrons drift in the azimuthal direction, with an average azimuthal velocity E_z/B_r. Typical values of the axial electric field E_z are on the order of 10^4 V/m, and the radial magnetic density B_r is 0.02 T, leading to average electron energies higher than 10 eV. This magnetically confined electron efficiently ionizes the propellant gas. Ions are accelerated toward the exit by the electric field, which produces the thrust for the satellite.

The plasma instability is inevitable in magnetic-confined plasma discharge of Hall thrusters. Past research has shown that regardless of the magnetic topology used, a highly rich and complex wave and noise characteristics over a wide frequency spectrum are inherent in the magnetic-confined plasma discharge. Therefore, to study all kinds of plasma instability, clarify the physical mechanism, understand their characteristics, and seek a stabilization method have always been the central issues of plasma physics [1–6]. Hall thrusters, as typical magnetized plasma discharge devices, exhibit varied oscillations with different lengths and time scales related with various physical processes. These oscillations play a major role in the process of ionization, diffusion, and acceleration of the particles. Low-frequency oscillations in the range of 10–100 kHz, also called breathing mode oscillations in some references, are among the major research topics of Hall thrusters [7, 8]. The typical low-frequency oscillation wave is shown in **Figure 2**. These oscillations might affect the reliability of power processing unit, reduce the efficiency and specific impulse of Hall thrusters, and therefore, its suppression is an essential challenge in the space applications of Hall thrusters not only to relate with the effects on the

http://dx.doi.org/10.5772/intechopen.71009

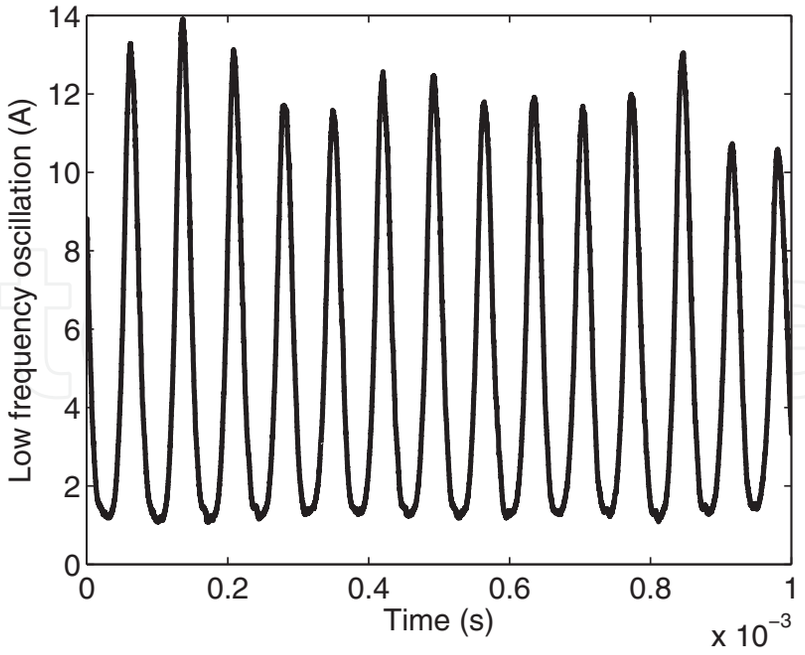

Figure 2. Typical low-frequency oscillation wave.

thruster operation but also to control electromagnetic compatibility with other equipment installed on satellites [9, 10]. Researchers have recognized the low-frequency oscillation phenomena with Hall thrusters since the early 1970s [11]. Even now, research on this subject is ongoing [12].

2. Research groups for plasma instability

In the world, there are many electric propulsion research groups, such as the Princeton Plasma Physics Laboratory (PPPL) in the U.S., the LAPLACE (Laboratory on Plasma and Conversion of Energy) in France, the Komurasaki-Koizumi Laboratory in Japan, the Moscow Institute of Radio-Engineering in Russia, and other laboratories in Asia and Europe. Some studies of low-frequency oscillation were performed in Russia in the early and mid-1970s; the main research groups continuing to study this subject are located in the U.S., France, Poland, Japan, and China. These groups have researched this subject from different angles and contributed to a full understanding of low-frequency oscillations in Hall thrusters.

In the U.S., studies on low-frequency oscillations are conducted mainly in universities. In PPPL, their research objectives include reducing beam divergence, scaling Hall thrusters, and studying the physics involved in Hall thrusters, as well as plasma instabilities and their control [13–16]. They have studied low-frequency oscillations experimentally and have established some excellent plasma diagnostics devices, included a high-speed positioning system for inside measurements, a movable radial probe, and a segmented probe [17–20]. Another research group at Princeton is EPPDyL (Electric Propulsion and Plasma Dynamics Lab), which has studied the physics and applications of plasma thrusters for more than 30 years. A review

of plasma oscillations in Hall thrusters published in *Physics of Plasmas* is their typical oscillation research work [21]. Plasmadynamics and Electric Propulsion Laboratory (PEPL) founded and directed by Gallimore in University of Michigan has operated all thruster types, including electrostatic thrusters, electrothermal propulsion, and electromagnetic thrusters. A majority of the research presently performed at the PEPL lies in Hall thrusters and ion thrusters [22]. In addition, the Stanford Plasma Physics Lab and the Space Propulsion Laboratory at the Massachusetts Institute of Technology are also advancing theoretical and experimental study on plasma physics and space propulsion, including the low-frequency oscillations.

In Europe, the groups focusing on low-frequency oscillations in Hall thrusters are mainly located in Poland and France. In France, Hall thrusters have been studied in the frame of a Research Group on Plasma Propulsion consisting of about 10 academic labs that specialize in all fields of Hall thruster physics (such as plasma physics, optical diagnostics, magnetism, ceramics, and numerical simulation). LAPLACE at the University of Toulouse and the Research Group on Ionized Media (GREMI) at Orléans University, headed by A. Bouchoule, are two of the most important research groups. These two groups have performed many theoretical and experimental studies on discharge instabilities of Hall thrusters in a wide frequency range. Barral is one of the most active researchers in Hall thruster discharge instability for the past few years [8, 23–26]. His work is mainly focused on modeling of plasma instability, discharge instabilities theory, and interactions between thruster and power supply. He has done much research and provided some new perspectives on low-frequency oscillations. Moreover, the Space Propulsion and Plasmas (EP2) research group in Spain, headed by E. Ahedo, has also performed some theoretical studies on the subject of discharge oscillations in Hall thrusters. EP2 has built research relationships with SPL, PPPL, and the Dynamics of Ionized Media group concerning the fundamental physics of Hall thrusters [24, 26–28].

The works of the Komurasaki-Koizumi Laboratory at the University of Tokyo include developing model and improving the characteristics and suppressing low-frequency oscillations [7, 29]. The works of the Gas Discharge Physics Lab in the Korea mainly focus on cylindrical type Hall thrusters and plasma diagnostics [30, 31]. The Harbin Institute of Technology Plasma Propulsion Laboratory (HPPL) in China is a new research group, which began to study Hall thrusters in 2004. They have done some exploratory research on low-frequency oscillations, including the influencing factors, physical mechanism, and stabilization [4, 10, 32–37].

In addition to these research centers, some researchers in Japan (such as Nagoya University and Gifu University) [38], Israel (such as in Technion Israel Institute of Technology and Holon Institute of Technology) [39, 40], and the U.S. (such as the Air Force Institute of Technology) [41], among others, also perform some research work on the subject of low-frequency oscillations in Hall thrusters.

3. Model and physical mechanism of low-frequency oscillation

The mechanism of low-frequency oscillations is usually explained using a predator-prey model. In this model, the ions and neutrals in an ionization zone can be expressed as

$$\frac{dn_i}{dt} = \beta n_i n_n - n_i \frac{V_i}{L_{ion}}$$
$$\frac{dn_n}{dt} = -\beta n_i n_n + n_n \frac{V_n}{L_{ion}} \tag{1}$$

where n_i and n_n are the ion number density and neutral number density, respectively. L_{ion} is the length of the ionization zone. Neutrals enter the ionization zone at a rate $n_n V_n$, but few neutrals leave. Ions leave the ionization zone at a rate $n_i V_i$, but few ions arrive. Ionization occurs at the rate of $\beta n_i n_n$. Results show that the n_i and n_n oscillate in an opposed-phase form, which indicates that the ions and neutrals have the relationship of predator and prey.

Although this model can reflect the complex processes of low-frequency oscillations, its boundary conditions are unreasonable. We investigate the meaning of the term $n_n V_n / L_{ion}$. In the original predator-prey model, it means without the existence of the predator, the growth rate of the prey is proportional to its own numbers. In the ionization model, it implies that the rate of neutrals entering the ionization zone is proportional to the number density of neutrals in the ionization zone, when in fact, neutrals are introduced into the channel at a constant rate. If the rate of neutrals arriving is fixed, the system would be stable unconditionally. Detailed calculation results are shown in [42].

It shows that the boundary conditions of the predator-prey model have a significant effect on system stability, which is unreasonable. In order to give reasonable boundary conditions, we can use the simplified equation set to reflect the characteristics of low-frequency oscillations. The predator-prey model is derived from the ion continuity equation and the neutral continuity equation. We begin with the following equation set:

$$\frac{\partial n_n}{\partial t} + \frac{\partial n_n V_n}{\partial x} = -\beta n_n n_i \tag{2}$$

$$\frac{\partial n_i}{\partial t} + \frac{\partial (n_i V_i)}{\partial x} = \beta n_n n_i \tag{3}$$

$$\frac{\partial (n_i V_i)}{\partial t} + \frac{\partial \left(n_i V_i^2\right)}{\partial x} = \frac{e n_i}{m_i} E(x) + \beta n_n n_i V_n \tag{4}$$

where the channel length is $\mathbf{L = 3\ cm}$, channel cross section is $\mathbf{A = 25\ cm^2}$, neutral velocity is $V_n = \mathbf{200\ m/s}$, and ionization rate is $\beta = \mathbf{5 \times 10^{-13}\ m^3/s}$. With operating conditions of a neutral gas flow rate of 3.0 mg/s and pre-ionization rate of 1% (the ionization rate of the neutral gas before entering the channel), the boundary conditions at the anode (x = 0) are $n_n(0, t) = \mathbf{2.6 \times 10^{19}\ m^{-3}}$, $V_i(0, t) = \mathbf{2000\ m/s}$, and $n_i(0, t) = \mathbf{2.6 \times 10^{16}\ m^{-3}}$. The values of $n_n(x, 0)$, $n_i(x, 0)$, $V_n(x, 0)$, and $E(x)$ are given according to a one-dimensional steady quasi-neutral hybrid model.

Simulation results show that the system is stable. The traces of n_i and n_n in the ionization zone are shown in **Figure 3** (we define the ionization zone as the region where n_i and n_n changes from 5–90%). The results show that even with equation set (2)–(4), the mechanism of ionization oscillations is incomplete. Further, we introduce the dynamic electric field as follows:

$$E = \frac{en_eV_e}{\sigma(x)} = \frac{I/A - en_iV_i}{\sigma(x)} \tag{5}$$

$$\int_0^L Edx = U_0 \tag{6}$$

where the discharge voltage is $\boldsymbol{U_0 = 300\ V}$. Electronic conductivity $\boldsymbol{\sigma(x)}$ depends only on the transverse magnetic field, which is given by $\boldsymbol{\sigma(x) = \sigma_0(H_0/H(x))^2}$, $\boldsymbol{\sigma_0 = 8.3 \times 10^{-3}\ S/m}$, and $\boldsymbol{H_0 = 0.02\ T}$. $\boldsymbol{H_0}$ is the magnetic field at the cathode, and $\boldsymbol{H(x)}$ is the profile of the transverse magnetic field. $\boldsymbol{\sigma_0}$ is the mean conductivity. The details of the parameter values and model can be found in [**43**]. With this model, the discharge current fluctuates at a frequency of approximately 30 kHz. In addition, the $\boldsymbol{n_i}$ and $\boldsymbol{n_n}$ change with discharge current (**Figure 4**). The results show that low-frequency oscillations are related with the changes of electric field.

From the view of the physical mechanism, the physical processes of low-frequency oscillations are shown in **Figure 5**. Because the rates of neutrals leaving ($\boldsymbol{n_nV_n}$) and ions arriving ($\boldsymbol{n_{i\_i}V_{i\_i}}$) are small, the main processes in the ionization zone are neutrals arriving at the rate of $\boldsymbol{n_{n\_i}V_n}$, ionization at the rate of $\boldsymbol{\beta n_in_n}$, and ions leaving at the rate of $\boldsymbol{n_iV_{i\_o}}$ (marked with the oval in **Figure 5**). For a fixed electric field, the ions acceleration characteristic is fixed. If a disturbance occurs in the ionization process and the ionization intensity increases, the $\boldsymbol{n_n}$ would decrease and the rate of ions leaving would be increased; the effects of these two processes cause the system balance again. When the time-dependent electric field is involved, the ionization process disturbance would be followed by a various ion momentum $\boldsymbol{n_iV_{i\_o}}$, and this change would affect the ion momentum in the acceleration zone. From Eq. (5), the change of ion

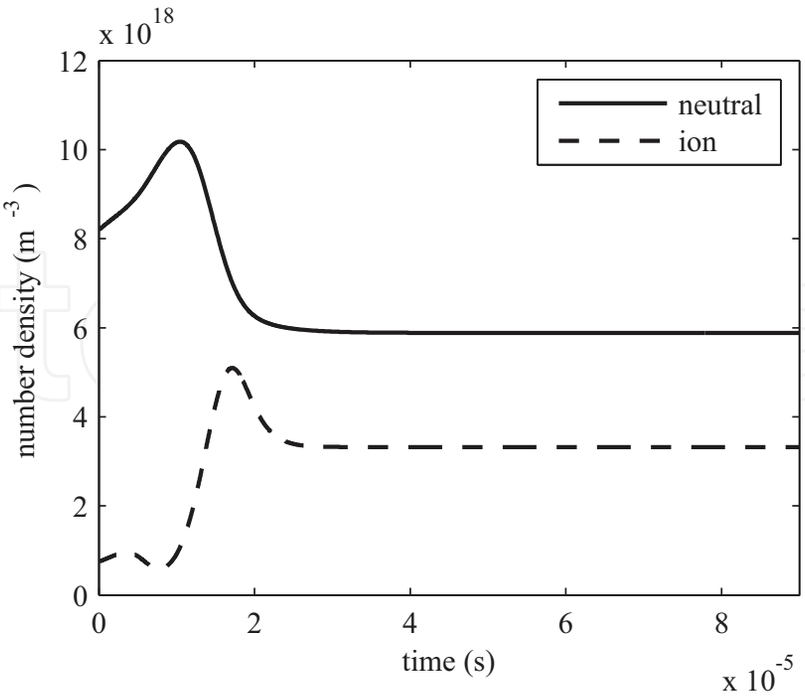

Figure 3. Changes in mean neutral number density and mean ion number density in the ionization zone with a constant electric field.

http://dx.doi.org/10.5772/intechopen.71009

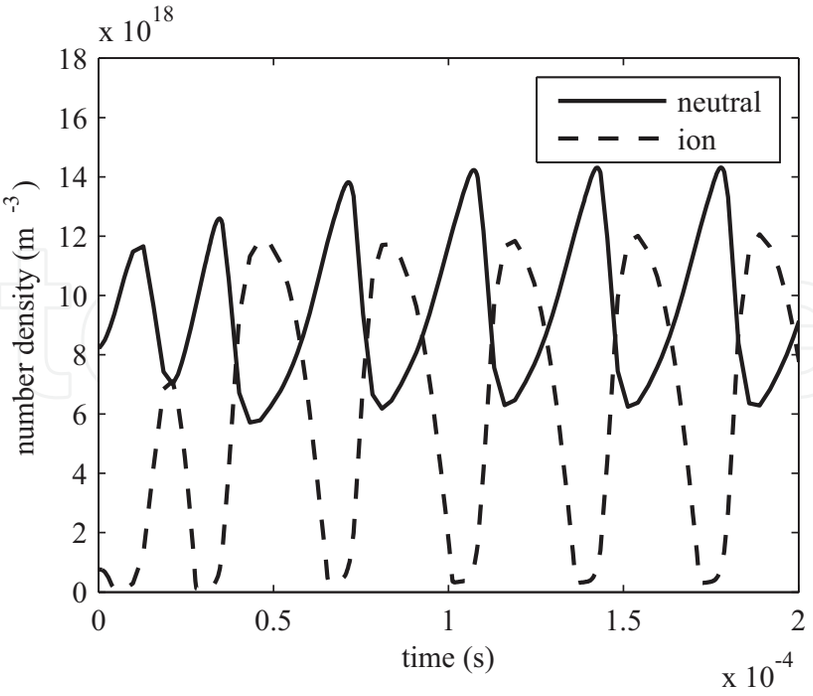

Figure 4. Changes in mean neutral number density and mean ion number density in the ionization zone with a dynamic electric field.

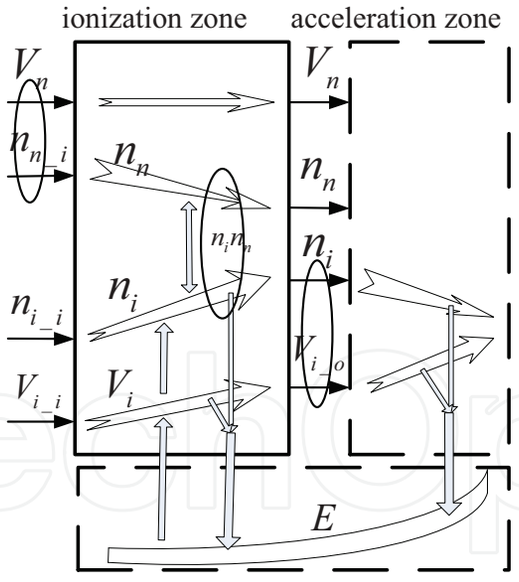

Figure 5. Physical processes of low-frequency oscillations.

momentum in the channel would cause the redistribution of the electric field, which influences the ion movement in the ionization zone again. The numerical results show that the feedback of the electric field, together with the replenishment and ionization avalanche of neutral, brings the oscillation. Analyzing particle movement process, the ionization zone is upstream of the acceleration zone. Electrons go into the ionization zone from the acceleration zone. The ionization zone and acceleration zone interact with each other due to this movement. The

electric field equation is essentially the electron momentum equation which reflects the interact between the acceleration zone and the ionization zone. Therefore, the import of a dynamic electric field makes the system into whole. The dynamic electric field is a highly important influence factor for low-frequency oscillation. The dynamic electric field is also applied and studied in many research areas, and these research results shown in the electric field have a plentiful scientific connotation [44–58].

4. Stabilizing low-frequency oscillation

The stabilizing method of low-frequency oscillation is an essential challenge for the space applications of thrusters. Researchers have tried many different ways to mitigate low-frequency oscillations. A filter, sometimes also called a matching network, is a component mainly applied to reduce the discharge current low-frequency oscillations in the range of 10–100 kHz; it is also an important component in the space mission of a Hall thruster. Previous studies indicated that the low-frequency oscillations are sensitive to filter parameters and can be mitigated to an acceptable level with proper filter values [59]. A filter unit is always involved between the thrusters and the power supply. The traditional filter consists of an inductor and a capacitor, and sometimes a resistor is also applied. This type of filter is a low-pass filter designed to isolate the interfering signal from the thrusters to the power supply. Recently, the role of the filter in the oscillation control was introduced by Yu et al. [4, 10, 33] and Barral et al. [25, 26]. It is noted that the filter regulates the voltage across itself according to the variation of discharge current so as to decrease its fluctuation in the discharge circuit, which is the function of a controller. Therefore, the matching network between the thrusters and power supply has two functions, which are those of a filter and controller. However, it is highly difficult to mix the function of a filter and controller in one network, because the aim and function of these two parts are quite different. This may be the reason that there have been no design methods of the matching network until now. The parameters are in practice always obtained through a trial-and-error method. Therefore, it follows that we should separate the matching network into two stages. The first stage is the filter, which aims to isolate the interfering signal from the thrusters to the power supply. The second stage is the controller, which provides a regulated voltage to decrease the low-frequency discharge current oscillation.

4.1. Design of the filter stage

As a matching network between the thruster and power supply, the function of a filter is to protect the power supply, that is, to obtain a stable load for the power supply and, therefore, enable the power supply to operate in its normal electrical state. Another requirement is that the filter has low insert impedance. In a manner of speaking, the design goal is to ensure stable current or voltage on the power supply side, even though the current fluctuates on the thruster side. The filter can be seen as a two-port network: the power supply provides constant input power, and the thruster consumes it with a frequency of 20–40 kHz. Thus, from the point of view of energy conservation, the filter needs a capacitor large enough to store energy and release it to a fluctuating load. Connecting the capacitor between the

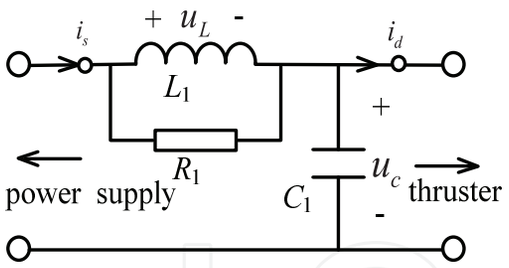

Figure 6. Configuration of the filter stage.

positive and negative terminals of the power supply directly may be unreasonable, because there will be a large current peak in the circuit when the power supply is turned on. Therefore, designers must choose a component to connect between the capacitor and the power supply, with the aim of charging the capacitor. This chosen component should have low DC impedance because it is connected in the discharge circuit. Moreover, the component should have high AC impedance. The reason can be understood as follows: The thruster consumes power with a pulsating mode, which would cause fluctuation in the capacitor voltage. The voltage difference between the power supply port and the thruster port would draw a fluctuating current from the power supply, and we do not expect that situation to occur. Thus, the component should have high AC impedance to suppress this kind of current fluctuation. Obviously, the component meeting these criteria is an inductor. Therefore, the filter stage consists of an inductor and a capacitor. On the thruster side, we use specific properties of charge storage to stabilize the discharge voltage, and on the power supply side, we use the inductor to achieve constant current. In order to avoid the LC circuit resonance and electromagnetic interference after extinguishing the thrusters, a resistor is connected parallel with the inductor. That is, the typical configuration of the filter stage is as shown in **Figure 6**.

According to the preceding analysis, the inductor in the filter stage should be sufficiently large to achieve a small power supply current fluctuation. On the other hand, the capacitor should be sufficiently large to ensure a small thruster voltage fluctuation. According to Fourier analysis, a fluctuating signal can be expressed as summation of different frequency components. Therefore, the supply current can be expressed as

$$i_s = \sum_i^n I_s^{(i)} \sin\left(2\pi f_i t + \varphi_i\right) \tag{7}$$

where $\boldsymbol{I_s^{(i)}}$ is the amplitude of the fluctuating current with frequency $\boldsymbol{f_i}$ and phase angle $\boldsymbol{\varphi_i}$. If we temporarily neglect to consider the existence of the resistor, the inductor voltage can be expressed as

$$u_L(t) = \sum_i^n 2\pi f_i L_1 \cdot I_s^{(i)} \cos\left(2\pi f_i t + \varphi_i\right) \tag{8}$$

According to electric circuit theory, the capacitor voltage can be expressed as

$$u_C(t) = \int \frac{1}{C_1}(i_d(t) - i_s(t))dt \tag{9}$$

where $\boldsymbol{i_d(t)}$ is the discharge current between the filter stage and the thruster as shown in **Figure 1**. Additionally, we introduce the Fourier analysis method, and therefore, Eq. (9) can be written as

$$u_C(t) = \int \frac{1}{C_1}\sum_i^n \left(I_d^{(i)}(t)\, sin\left(2\pi f_i t + \theta_i\right) - I_s^{(i)}(t)\, sin\left(2\pi f_i t + \varphi_i\right)\right)dt \tag{10}$$

$$u_C(t) = \sum_i^n \frac{1}{2\pi f_i C_1}\left(I_s^{(i)}(t)\, sin\left(2\pi f_i t + \varphi_i\right) - I_d^{(i)}(t)\, sin\left(2\pi f_i t + \theta_i\right)\right) \tag{11}$$

According to Kirchhoff's law and taking into account the requirement of a small thruster voltage fluctuation, the sum of capacitor voltage and the inductor voltage fluctuation should be zero. Thus, we obtain

$$|u_C(t)| = \left|\sum_i^n \frac{1}{2\pi f_i C_1}\left(I_s^{(i)}(t)\, sin\left(2\pi f_i t + \varphi_i\right) - I_d^{(i)}(t)\, sin\left(2\pi f_i t + \theta_i\right)\right)\right| = |u_L(t)| \tag{12}$$

Substituting Eq. (8) into Eq. (12) yields

$$\left|\sum_i^n \frac{\left(I_s^{(i)}(t)\, sin\left(2\pi f_i t + \varphi_i\right) - I_d^{(i)}(t)\, sin\left(2\pi f_i t + \theta_i\right)\right)}{2\pi f_i C_i}\right| = \left|\sum_i^n 2\pi f_i i_s^{(i)}\, cos\left(2\pi f_i t + \varphi_i\right)\right| \tag{13}$$

As is well known, the phase angle of an ideal inductor voltage leads its current by 90°, and the phase angle of an ideal capacitor voltage lags its current by 90°, an ideal voltage source equivalent to a line in an AC circuit. Therefore, the phase relationship between $\boldsymbol{u_L}$ and $\boldsymbol{u_C}$ is opposite. The phase relationship between $\boldsymbol{i_s}$ and $\boldsymbol{i_C}$ is also opposite. Considering that $\boldsymbol{i_d}$ is the sum of $\boldsymbol{i_s}$ and $\boldsymbol{i_C}$, the phase angle of $\boldsymbol{i_s}$ and $\boldsymbol{i_d}$ is equal to 180°. That is, $\boldsymbol{\theta_i}$ and $\boldsymbol{\varphi_i}$ in Eq. (13) have a phase-angle difference of 180°. However, it is highly difficult to simplify Eq. (13) with all frequency components because of the limitation of the mathematical equivalence relation. From the angle of decrease for the low-frequency oscillation, it is also unreasonable to consider waves of all frequencies to set the parameters of the inductor and capacitor. Thus, we simply take into account the main frequency component as low-frequency oscillation $\boldsymbol{f_0}$. The goal of the design is that the power supply current fluctuation is one part per $\boldsymbol{\alpha}$ of the thruster current fluctuation, which means $\boldsymbol{I_s = \frac{1}{\alpha} I_d}$. The inductor and capacitor of the filter stage must satisfy

$$L_1 C_1 = \frac{\left|\frac{1}{2\pi f_0}(1-\alpha)\, cos\left(2\pi f_0 t + \delta_0\right)\right|}{\left|2\pi f_0\, cos\left(2\pi f_0 t + \varphi_0\right)\right|} \tag{14}$$

where $\boldsymbol{\delta_0}$ is the vector resultant angle of the power supply current and thruster current. $\boldsymbol{\alpha}$ can be represented as the current attenuation ratio. Eq. (14) can be also simplified to

$$L_1 C_1 = \frac{|(1-\alpha)\gamma|}{|4\pi^2 f_0^2|}. \tag{15}$$

Here, the parameter γ represents the effects of the phase angles $\boldsymbol{\delta_0}$ and $\boldsymbol{\varphi_0}$. Obviously, it is difficult to obtain the value of γ, but we can estimate the range of its value. φ_0 is the phase angle of the inductor current, and $\boldsymbol{\delta_0}$ is the vector resultant angle of the power supply current and thruster current. According to the analysis of the phase relationship in [45], the phase angle difference between $\boldsymbol{\delta_0}$ and $\boldsymbol{\varphi_0}$ is equal to 180°. Thus, $\gamma = \frac{\cos\delta_0}{\cos\phi_0}$ and its value is approximately −1. For example, if we want to ensure that the ripple current of the power supply is one-tenth the thruster current fluctuation, then $\boldsymbol{\alpha}$ is larger than or equal to $\boldsymbol{\alpha_0}$=**10**. The frequency of the low-frequency oscillation is assumed to be 20 kHz. Under these assumptions, the product of the inductance and capacitance should be greater than or equal to 5.7×10^{-10}. If we choose the inductance to be 0.1 mH, the capacitance should be greater than 5.7 μF. The inductance and the capacitance values could be different combinations as long as they satisfy Eq. (9). However, the value of the inductor and capacitor should also take certain factors into consideration, such as the DC power dissipation, volume, and weight. After the determination of the inductance and capacitance, it can be seen that an LC network would have a resonant peak in its characteristic frequency. This would induce undesired electromagnetic interference. Thus, a resistor is usually connected in parallel with the inductor. Under normal conditions, the resistance is in the range 50–200 Ω. Excessive resistance will cause the damping coefficient to be too small, and the electromagnetic interference will increase. Undervalued resistance will weaken the effects of the inductor and cause an increase in power supply current fluctuation. Thus, the resistance of the resistor is often chosen on the basis of experiments.

Figure 7 shows a contour plot of the current attenuation ratio $\boldsymbol{\alpha}$, with different inductance and capacitance values. It can be seen that the current attenuation ratio increases with the increase in inductance and capacitance in the filter stage. Though the larger inductance and capacitance yields a larger current attenuation ratio, it is also accompanied by an increase in the capacitor volume and inductor weight. Therefore, the reasonable range of current attenuation ratio is approximately 5–10.

4.2. Design of the controller stage

From the view of control theory, a thruster, discharge power supply, and filter can be seen as a feedback control system as shown in **Figure 8**. In this system, the Hall thruster is the controlled object, the discharge power supply voltage is the reference signal, and the filter is the controller. Therefore, we designate the filter stage as the controller stage. The controller stage filter regulates the voltage across itself according to the variation of discharge current, so as to affect the electric field distribution in the discharge channel and therefore decrease the discharge current fluctuation in the discharge circuit [8, 10, 12, 26, 33]. The simplest component that can provide a varying voltage with a change in current is an inductor. However, the magnetized plasma of a Hall thruster exhibits varied oscillations ranging from kilohertz to gigahertz. High-frequency current oscillation will cause an undesirable high-amplitude oscillation of the inductor voltage. Thus, we require the controller stage to have sufficient gain in the low band but to decay the signal in the high-frequency band. The required frequency response characteristics

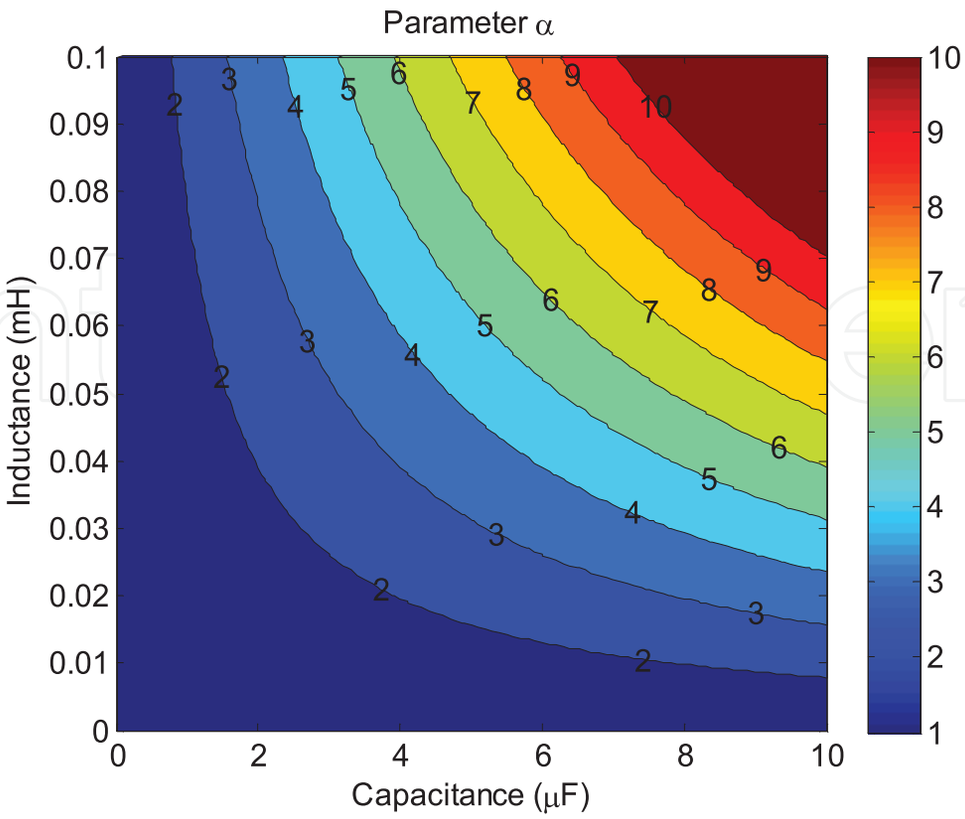

Figure 7. Contour plot of the current attenuation ratio α, with different inductance and capacitance values.

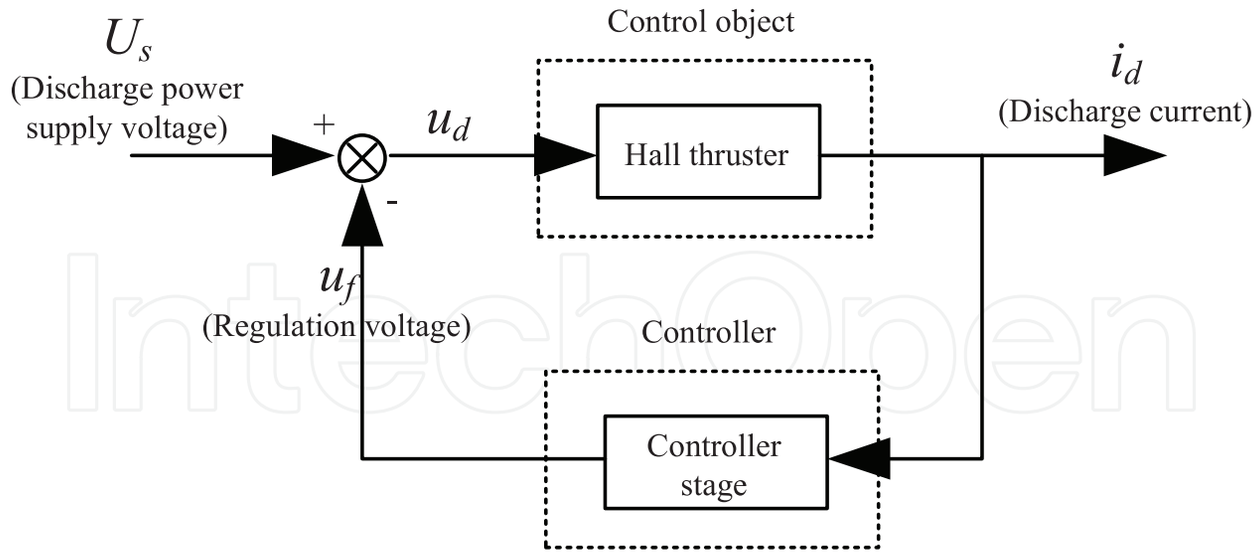

Figure 8. Schematic diagram of the feedback control system for Hall thrusters.

would look like that shown in **Figure 9**. According to control theory, it is a typical second-order system that can be realized by the network (controller stage) shown in **Figure 10**. If we consider the oscillation current as the input signal and the voltage of the control filter stage (the voltage at the thruster) as the output signal, the transfer function can be expressed as

http://dx.doi.org/10.5772/intechopen.71009

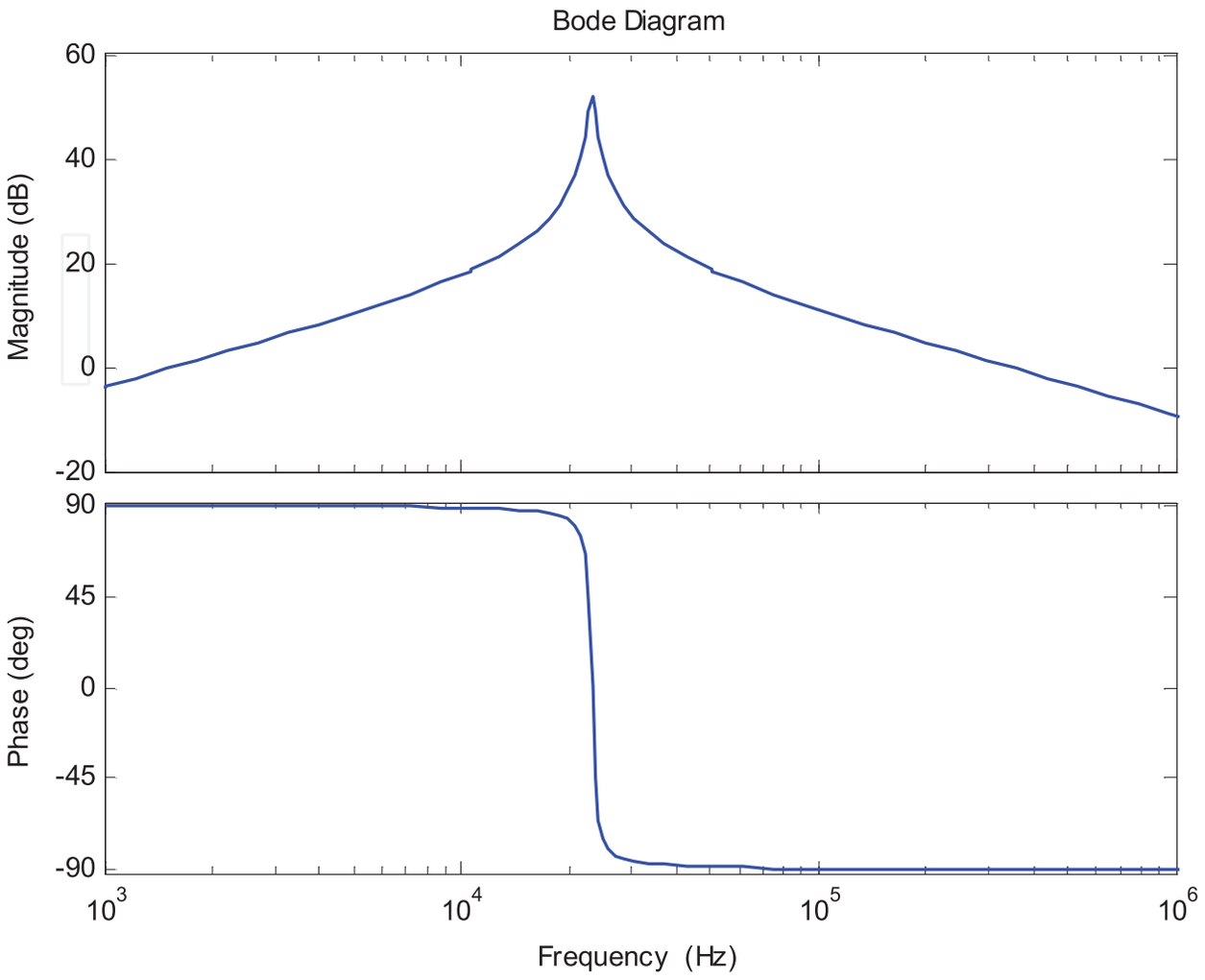

Figure 9. Schematic diagram of the ideal frequency response characteristics of the controller stage.

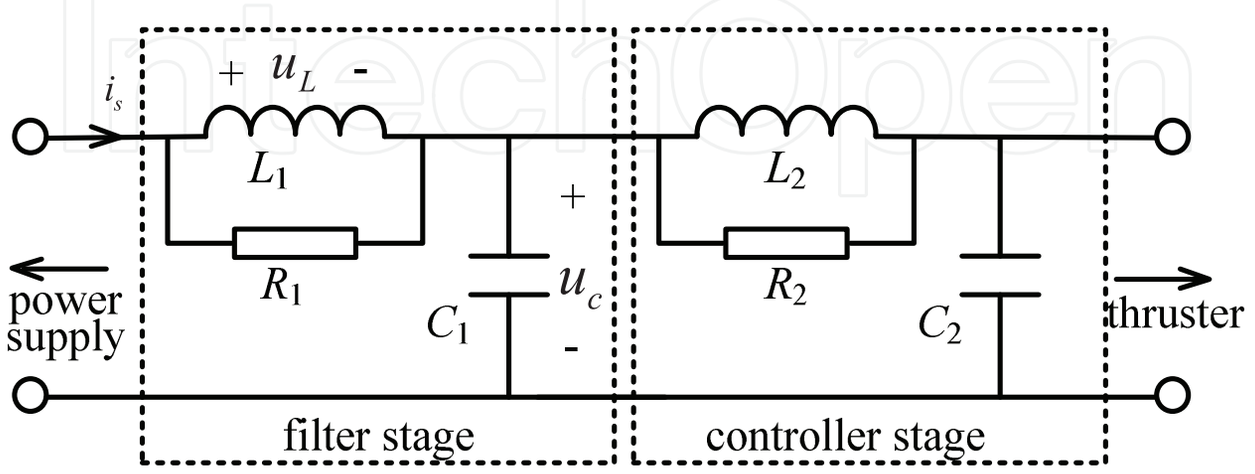

Figure 10. Schematic diagram of the two-stage filter for Hall thrusters.

$$\Phi(s) = \frac{K\omega_n^2 s}{s^2 + 2\omega_n \xi s + \omega_n^2} \tag{16}$$

where $K = L_2$, $\omega_n = \frac{1}{\sqrt{L_2 C_2}}$, $\xi = \frac{1}{2R_2}\sqrt{\frac{L_2}{C_2}}$, and s is the Laplacian operator. Obviously, the parameters of the controller stage relate to the required gain of the system. If we suppose the minimum gain is g_0 with the low-frequency oscillation frequency f, it must satisfy

$$20\lg\left(\Phi(s)|_{s=j\omega}\right) = 20\lg\left|\frac{K\omega_n^2 j\omega}{(j\omega)^2 + 2\omega_n \xi \cdot j\omega + \omega_n^2}\right| = 20\lg\left|\frac{2\pi f L_2 R_2 j}{2\pi f L_2 j - 4\pi^2 f^2 R_2 L_2 C_2 + R^2}\right| \geq g_0 \tag{17}$$

Rewriting Eq. (17), we obtain

$$\frac{2\pi f R_2 L_2}{\sqrt{\left(R_2 - 4\pi^2 f^2 R_2 L_2 C_2\right)^2 + (2\pi f L_2)^2}} = 10^{\frac{g_0}{20}}. \tag{18}$$

Considering the turnover frequency of the system is

$$f_z = \frac{1}{2\pi\sqrt{L_2 C_2}}, \tag{19}$$

Eq. (18) can be expressed as

$$\frac{\left(1 - \left(\frac{f}{f_z}\right)^2\right)^2}{(2\pi f L_2)^2} - \frac{1}{R_2^2} = 10^{-\frac{g_0}{10}}. \tag{20}$$

The resistor affects only the gain near the turnover frequency, and thus, we temporarily ignore the effects of the resistor. We then obtain

$$L_2 = 10^{\frac{g_0}{20}} \cdot \frac{1 - \left(\frac{f}{f_z}\right)^2}{2\pi f}. \tag{21}$$

Considering Eq. (19), we therefore know that the capacitance must satisfy

$$C_2 = 10^{-\frac{g_0}{20}} \cdot \frac{f}{2\pi\left(f_z^2 - f^2\right)} \tag{22}$$

A proper filter parameter can provide a regulated voltage with a suitable amplitude and phase angle to control the oscillation of plasma density in the channel so as to decrease the current oscillation in the discharge circuit. Though it is difficult to determine the phase angle of plasma density in the ionization region, the phase relationship between the discharge current and the plasma density in the ionization region can be obtained by analyzing the propellant ionization process in the discharge channel. When the propellant is ionized in the ionization region, the plasma density in the ionization region reaches its highest point. Subsequently, the produced ions are accelerated to their high velocity in the accelerating region, and the discharge current

reaches its maximum. From the analysis of the propellant ionization process, it can be seen that there is a lag of time between the discharge current and the plasma density of the ionization region in the time scale of low-frequency oscillation. Thus, when the plasma density in the ionization region increases, the control stage filter should provide a voltage to balance the large ion production. Thus, the regulated voltage of the filter has a phase-angle difference from the discharge current. According to the accelerated time of ions in the discharge channel, the phase-angle, δ, should be in the range of 0–90°. This phase angle can be provided by the resistor paralleled between the inductors. From circuit theory, for the designed filter, the phase angle between the voltage and current can be calculated by

$$\tan\delta = 2\pi f R_2 C_2 - \frac{R_2}{2\pi f L_2}. \tag{23}$$

Substituting Eqs. (21) and (22) into Eq. (23) enables the resistance to be estimated by

$$R_2 = 10^{\frac{g_0}{20}} \cdot \tan\delta, \tag{24}$$

where δ is the phase angle between the regulated voltage and the discharge current. This phase angle is estimated in the range of 0–90°, which would affect the variation of the electric field and therefore help to balance the ion production.

The discharge circuit of a Hall thruster can be seen as a feedback control system. The controller stage regulates the voltage across itself according to the variation of discharge current, so as to decrease its fluctuation in the discharge circuit. As the ion number density increases, the ionization production becomes larger than the number of ions being ejected. A high discharge voltage is helpful for balancing the large ion production by increasing the ion mobility. When the ion number density decreases, a relatively small discharge voltage will decrease the ion mobility and help balance the ion production. According to Eq. (17), the minimum gain is the logarithm transformation of the ratio between the minimum fluctuating discharge voltage and the fluctuating discharge current. Here, the minimum fluctuating discharge voltage is the voltage to balance the fluctuating discharge current at that time. That is, the physical meaning of the minimum gain is the voltage provided by the controller stage to stabilize the unit current oscillation. Obviously, it is almost impossible to determine the exact minimum gain for various discharge operating conditions. However, we also can determine some useful reference values for the minimum gain along with experimental testing and analysis. We can calculate the RLC parameters in the controller stage under different gains and turnover frequencies of the system as shown in **Figure 11** according to Eqs. (21)–(23). It can be seen that the inductance increases with increasing given system gain and turnover frequency, and the capacitance decreases with increasing given system gain and turnover frequency. The choice of turnover frequency has no effect on the resistance of the resistor. The resistance increases only with the increase in given system gain.

Keeping the turnover frequency unchanged, we choose the RLC parameters to obtain different system gains. The relationships between the standard deviation of low-frequency oscillations and system gain with a confidence coefficient of 95% are shown in **Figure 12**. As the system gain increases, the standard deviation of the discharge current low-frequency oscillations measured on the thruster side with a current probe declines and then slightly increases. When

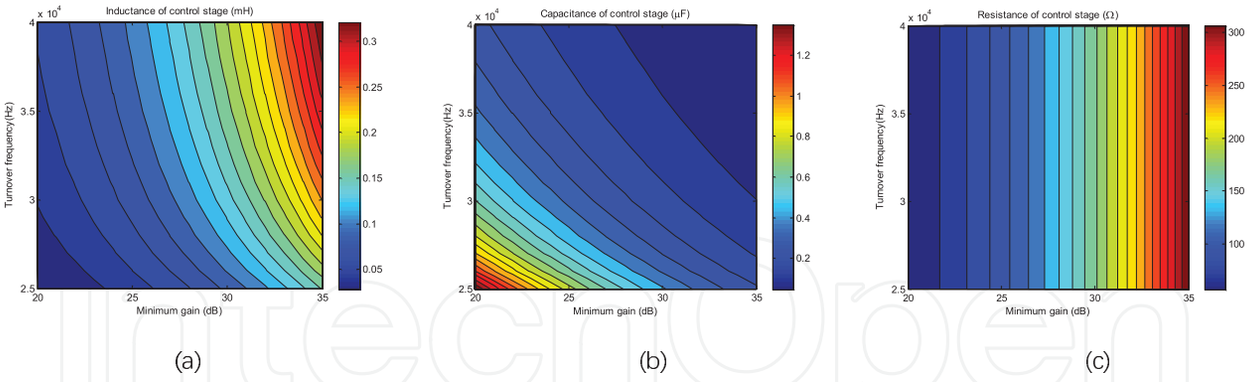

Figure 11. RLC parameters under different gains and turnover frequencies of the system: (a) Calculated results of inductance, (b) calculated results of capacitance, and (c) calculated results of resistance.

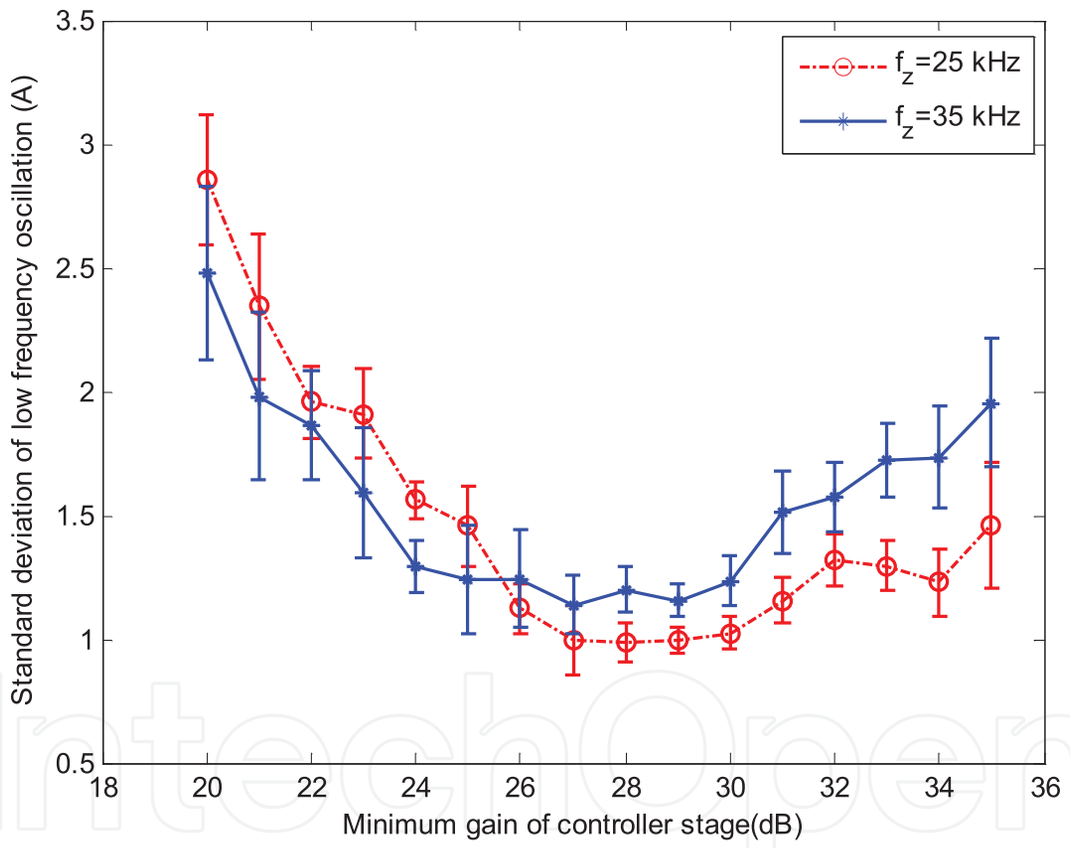

Figure 12. Standard deviation of low-frequency oscillation as a function of minimum gain of the controller stage.

the system gain is approximately 25–35 dB, the low-frequency discharge current oscillation reaches its minimum. When the system gain deviates from this range, the low-frequency discharge current oscillations will increase. This can be explained as follows: When the system gain is comparatively low, the provided regulated voltage is too small to stabilize the low-frequency oscillation. The discharge current oscillation thus increases. On the contrary, when the system gain is too high, the provided regulated voltage is excessive. The discharge current oscillation will increase as well. In other words, if the regulated voltage (system gain) is too

small or too large, the Hall thruster performs as over-regulated or inadequately regulated. Though the frequency of the low-frequency discharge current oscillations will vary with the discharge parameter, the variation is slight because of the mechanism of low-frequency oscillations. In addition, the controller stage is designed to have enough bandwidth in the range of the frequency of the low-frequency oscillations. Therefore, the variation in frequency may not affect the controllability of the controller stage. [10, 12, 33]

The analysis can also be verified by the experimental data for a turnover frequency 35 kHz as shown in **Figure 12**. The current oscillation in **Figure 12** was measured between the filter and thruster. As seen in **Figure 12**, when the turnover frequency is high, the bandwidth of the controller is widened. More high-frequency components in the discharge current across the control stage networks cause the controller to provide more regulated voltage. Therefore, in the range of low system gain, the low-frequency oscillation with $f_z = 35$ kHz is lower than that of $f_z = 25$ kHz. However, in the range of high system gain, the relation is the reverse. If we propose $g_0 = 30$ dB, $\delta = 80^\circ$, $f = 20$ kHz, and $f_z = 25$ kHz, we can therefore obtain the parameters of the controller stage as $R_2 = 179\ \Omega$, $L_2 = 0.09$ mH , and $C_2 = 0.447\ \mu$F. According to these experiments and analysis, it can be considered that a reasonable system gain is approximately 25–35 dB per unit current input, the output voltage can be expressed as

$$u = \frac{2\pi f R_2 L_2}{\sqrt{\left(R_2 - 4\pi^2 f^2 R_2 L_2 C_2\right)^2 + \left(2\pi f L_2\right)^2}} = 10^{\frac{g_0}{20}} \tag{25}$$

If we consider the required gain, g_0, is approximately 25–35 dB, the output voltage is in the range 17.78–56.23 V. Supposing that the length of the accelerated region is approximately 10 mm, the equivalent electric field strength increase or decrease for stabilizing a unit discharge current fluctuation is 1700–5600 V/m. We cannot give a precise physical explanation of why it needs this quantity of fluctuating electric field strength, because these are derived average control values. However, it can be evaluated that this fluctuating electric field strength will increase or decrease the average velocity of ions by 3–10%. For the experimental thruster with a 4-A mean discharge current, the unit discharge current fluctuation is roughly equivalent to the discharge current fluctuation in the range 87.5–112.5%. The fluctuation scale of the parameters seems to be reasonable.

Owing to the fact that the effects of the dynamic electric field on plasma instability are a highly complex subject, much work is expected to be done in this field in the future. The contribution of this work lies in the thought process, which is to separate the design of the filter into two stages. The first stage is a filter that aims to isolate the interfering signal from the thrusters to the power supply. This second stage is a controller, which provides a regulated voltage to decrease the low-frequency discharge current oscillation. The range of the parameters in the two stages is given according to the experiments and analysis. Finally, it should be noted that the design method of the two-stage filter works on the premise that the magnetic field of the thruster is reasonably designed. That is, the ionization zone should be controlled in a small region. The action of the controller stage might then be executed effectively [60].

Acknowledgements

Parts of this chapter are reproduced from authors' recent publication [4, 10, 12]. The authors would like to acknowledge the support of the National Natural Science Foundation of China (No. 51477035 and 51777045).

Nomenclature

A	Channel cross section
B_r	Radial magnetic density
C_1	Capacitance in filter stage
C_2	Capacitance in controller stage
E_z	Axial electric field strength
f	Fluctuating current frequency
f_0	Main frequency of low-frequency oscillation
f_z	Turnover frequency
g_0	Minimum gain is
H_0	Magnetic field at the cathode
i_d	Discharge current
$I_d^{(i)}$	Amplitude of discharge current with frequency f_i and phase angle θ_i.
i_s	Power supply current
$I_s^{(i)}$	Amplitude of power supply current with frequency f_i and phase angle φ_i
L	Channel length
L_1	Inductance in filter stage
L_2	Inductance in controller stage
L_{ion}	Ionization zone length
n_i	Ion number density
n_n	Neutral number density
R_1	Resistance in filter stage
R_2	Resistance in controller stage
s	Laplacian operator

u_L Inductor voltage

u_C Capacitor voltage

U_0 Discharge voltage

V_i Neutral number velocity

V_n Neutral number velocity

α Current attenuation ratio

β Ionization rate

δ Phase angle between the regulated voltage and the discharge current

σ_0 Mean conductivity of the channel

φ Power supply current phase angle

θ Discharge current phase angle

Author details

Liqiu Wei*, Yongjie Ding and Daren Yu

*Address all correspondence to: weiliqiu@163.com

Harbin Institute of Technology, Harbin, People's Republic of China

References

[1] Hitendra K. Malik and Sukhmander Singh. Resistive instability in a Hall plasma discharge under ionization effect. Physics of Plasmas. 2013;**20**(5):052115. DOI: http://dx.doi.org/10.1063/1.4804346

[2] Malik HK, Singh S. Conditions and growth rate of Rayleigh instability in a Hall thruster under the effect of ion temperature. Physical Review E. 2011;**83**(3):036406. DOI: 10.1103/PhysRevE.83.036406

[3] Boeuf JP, Garrigues L. Low frequency oscillations in a stationary plasma thruster. Journal of Applied Physics. 1998;**84**(7):3541-3554. DOI: http://dx.doi.org/10.1063/1.368529

[4] Liqiu W, Wang C, Zhongxi N, Weiwei L, ChaoHai Z, Yu D. Experimental study on the role of a resistor in the filter of Hall thrusters. Physics of Plasmas. 2011;**18**(6):063508. DOI: 10.1063/1.3599519

[5] Sukhmander Singh, Hitendra K. Malik. Role of ionization and electron drift velocity profile to Rayleigh instability in a Hall thruster plasma. Journal of Applied Physics. 2012;**112**(1):013307. DOI: http://dx.doi.org/10.1063/1.4733339

[6] Singh S, Malik HK. Growth of low-frequency electrostatic and electromagnetic instabilities in a Hall thruster. IEEE Transactions on Plasma Science. 2011;**39**(11):1910-1911. DOI: 10.1109/TPS.2011.2162652

[7] Yamamoto N, Komurasaki K, Arakawa Y. Discharge current oscillation in Hall thrusters. Journal of Propulsion and Power. 2005;**21**(5):870-876 https://doi.org/10.2514/1.12759

[8] Barral S, Kaczmarczyk J, Kurzyna J, Dudeck M. Closed-loop control of ionization oscillations in Hall accelerators. Physics of Plasmas. 2011;**18**(8):083504. DOI: 10.1063/1.3622655

[9] Tamida T, Nakagawa T, Suga I, Osuga H, Ozaki T, Matsui K. Determining parameter sets for low-frequency-oscillation-free operation of Hall thruster. Journal of Applied Physics. 2007;**102**(4):043304. DOI: 10.1063/1.2771039

[10] Liqiu W, Zhongxi N, Peng E, Daren Y. On the frequency characteristic of inductor in the filter of Hall thrusters. Journal of Vacuum Science and Technology A. 2010;**28**(5):L9-L13. DOI: 10.1116/1.3457152

[11] Morozov AI, Esipchuk YV, Kapulkin AM, Nevrovskii VA, Smirnov VA. Effect of the magnetic field on a closed-electron-drift accelerator. Soviet Physics: Technical Physics. 1972;**17**(3):482-487

[12] Li-Qiu W, Liang H, Yu D-R, Guo N. Low-frequency oscillations in Hall thrusters. Chinese Physics B. 2015;**24**(5):055201. DOI: 10.1088/1674-1056/24/5/055201

[13] Raitses Y, Smirnov A, Fisch NJ. Enhanced performance of cylindrical Hall thrusters. Applied Physics Letters. 2007;**90**(22):221502. DOI: 10.1063/1.2741413

[14] Granstedt EM, Raitses Y, Fisch NJ. Cathode effects in cylindrical Hall thrusters. Journal of Applied Physics. 2008;**104**(10):103302. DOI: 10.1063/1.2999343

[15] Smirnov A, Raitses Y, Fisch NJ. Controlling the plasma flow in the miniaturized cylindrical Hall thruster. IEEE Transactions on Plasma Science. 2008;**30**(5):1998-2003. DOI: 10.1109/TPS.2008.2002148

[16] Raitses Y, Smirnov A, Fisch NJ. Effects of enhanced cathode electron emission on Hall thruster operation. Physics of Plasmas. 2009;**16**(5):057106. DOI: 10.1063/1.3131282

[17] Staack D, Raitses Y, Fisch NJ. Shielded electrostatic probe for nonperturbing plasma measurements in Hall thrusters. Review of Scientific Instruments. 2004;**75**(2):393-399. DOI: 10.1063/1.1634353

[18] Polzin KA, Sooby ES, Raitses Y, Merino E, Fisch NJ. Discharge oscillations in a permanent magnet cylindrical Hall-effect thruster. In: 31st International Electric Propulsion Conference; September 20–24; Ann Arbor, MI. 2009. p. IEPC-2009-122

[19] Raitses Y, Parker JB, Fisch NJ. Plume narrowing and suppression of low frequency oscillations in cylindrical Hall thrusters. In: 31st International Electric Propulsion Conference; September 20–24; Ann Arbor, Michigan. 2009. p. IEPC-2009-123

[20] Parker JB, Raitses Y, Fisch NJ. Transition in electron transport in a cylindrical Hall thruster. Applied Physics Letters. 2010;**97**(9):091501. DOI: 10.1063/1.3486164

[21] Choueiri EY. Plasma oscillations in Hall thrusters. Physics of Plasmas. 2001;**8**(4):1411-1426. DOI: 10.1063/1.1354644

[22] Lobbia RB, Gallimore AD. Two-dimensional time-resolved breathing mode plasma fluctuation variation with Hall thruster discharge settings. In: Presented at the 31st International Electric Propulsion Conference; September 20–24, 2009; University of Michigan Ann Arbor, Michigan, USA. 2009. p. IEPC-2009-106

[23] Barral S, Peradzyński Z. Ionization oscillations in Hall accelerators. Physics of Plasmas. 2010;**17**(1):014505. DOI: 10.1063/1.3292645

[24] Barral S, Ahedo E. Low-frequency model of breathing oscillations in Hall discharges. Physical Review E. 2009;**79**(4):046401. DOI: 10.1103/PhysRevE.79.046401

[25] Barral S, Miedzik J. Numerical investigation of closed-loop control for Hall accelerators. Journal of Applied Physics. 2011;**109**(1):013302. DOI: 10.1063/1.3514151

[26] Barral S, Miedzik J. A model for the active control of low frequency oscillations in Hall. In: 44th AIAA/ASME/SAE/ASEE Joint Propulsion Conference & Exhibit; July 21–23, 2008; Hartford. 2008. p. AIAA 2008-4632

[27] Ahedo E. Plasmas for space propulsion. Plasma Physics and Controlled Fusion. 2011;**53**(18): 124037. DOI: 10.1088/0741-3335/53/12/124037

[28] Parraa FI, Ahedob E, Fifec JM, Martínez-Sánchez M. A two-dimensional hybrid model of the Hall thruster discharge. Journal of Applied Physics. 2006;**100**(2):023304. DOI: 10.1063/1.2219165

[29] Yamamoto N, Nakagawa T, Komurasaki K, Arakawa Y. Discharge plasma fluctuations in Hall thrusters. Vacuum. 2002;**65**(3–4):375-381. DOI: 10.1016/S0042-207X(01)00445-6

[30] Kim H, Lim Y, Choe W, Seon J. Effect of multiply charged ions on the performance and beam characteristics in annular and cylindrical type Hall thruster plasmas. Applied Physics Letters. 2014;**105**(14):144104. DOI: 10.1063/1.4897948], 10.1063/1.4897948]

[31] Lim Y, Kim H, Choe W, Lee SH, Seon J, Lee HJ. Observation of a high-energy tail in ion energy distribution in the cylindrical Hall thruster plasma. Physics of Plasmas. 2014;**21**(10): 103502. DOI: http://dx.doi.org/10.1063/1.4897178

[32] Liqiu W, Wang C, Ke H, Yu D. Effect of ionization distribution on the low frequency oscillations mode in Hall thrusters. Physics of Plasmas. 2012;**19**(1):012107. DOI: 10.1063/1.3676160

[33] Yu D, Wang C, Wei L, Gao C, Guang Y. Stabilizing of low frequency oscillation in Hall thrusters. Physics of Plasmas. 2008;**15**(11):113503. DOI: 10.1063/1.3023150

[34] Yu D, Wei L, Zhao Z, Han K, Yan G. Effect of preionization in Aton-type Hall thruster on low frequency oscillation. Physics of Plasmas. 2008;**15**(4):043502. DOI: 10.1063/1.2901196

[35] Wang C, Wei L, Ning Z, Daren Y. Effects of magnetic field strength on the low frequency oscillation in Hall thrusters. Physics of Plasmas. 2011;**18**(1):013507. DOI: 10.1063/1.3533915

[36] Liqiu W, Ke H, Chunsheng W, Li H, ChaoHai Z, Daren Y. Study on breathing mode oscillation suppression of self-excited Hall thrusters. Journal of Vacuum Science and Technology A. 2012;**30**(6):061304. DOI: 10.1116/1.4758788

[37] Wang C, Wei L, Daren Y. A basic predator-prey type model for low frequency discharge oscillations in Hall thrusters. Contributions to Plasma Physics. 2011;**51**(10):981-988. DOI: 10.1002/ctpp.201100040

[38] Miyasaka T, Shibata Y, Asato K. Particle simulation of discharge current oscillation in Hall thrusters. Vacuum. 2009;**83**(1):61-66. DOI: 10.1016/j.vacuum.2008.03.023

[39] Kapulkin A, Guelman MM. Low-frequency instability in near-anode region of Hall thruster. IEEE Transactions on Plasma Science. 2008;**36**(5):2082-2087. DOI: 10.1109/TPS.2008.2003359

[40] Fruchtmana A, Cohen-Zur A. Plasma lens and plume divergence in the Hall thruster. Applied Physics Letters. 2006;**89**(11):111501. DOI: 10.1063/1.2349827

[41] Liu D, Huffman RE, Branam RD, Hargus WA Jr. Ultrahigh-speed imaging of Hall-thruster discharge oscillations with Krypton propellant. IEEE Transactions on Plasma Science. 2011;**39**(11):2926-2927. DOI: 10.1109/TPS.2011.2146282

[42] Barral S, Peradzyn'ski Z. A new breath for the breathing mode. In: the 31st International Electric Propulsion Conference; September 20–24, 2009; University of Michigan, Ann Arbor, Michigan, USA. 2009. p. IEPC-2009-070

[43] Morozov AI, Savel'ev VV. One-dimensional hybrid model of a stationary plasma thruster. Plasma Physics Reports. 2000;**26**(10):934-939. DOI: 10.1134/1.1316827

[44] Sheikholeslami M. Influence of magnetic field on nanofluid free convection in an open porous cavity by means of Lattice Boltzmann method. Journal of Molecular Liquids. 2017;**234**:364-374. DOI: 10.1016/j.molliq.2017.03.104

[45] Sheikholeslami M. Magnetohydrodynamic nanofluid forced convection in a porous lid driven cubic cavity using Lattice Boltzmann method. Journal of Molecular Liquids. 2017;**231**:555-565. DOI: 10.1016/j.molliq.2017.02.020

[46] Sheikholeslami M. CuO-water nanofluid free convection in a porous cavity considering Darcy law. The European Physical Journal Plus. 2017;**132**:55. DOI: 10.1140/epjp/i2017-11330-3

[47] Sheikholeslami M. Magnetic field influence on nanofluid thermal radiation in a cavity with tilted elliptic inner cylinder. Journal of Molecular Liquids. 2017;**229**:137-147. DOI: 10.1016/j.molliq.2016.12.024

[48] Sheikholeslami M. Numerical simulation of magnetic nanofluid natural convection in porous media. Physics Letters A. 2017;**381**:494-503. DOI: 10.1016/j.physleta.2016.11.042

[49] Sheikholeslami M. Magnetic source impact on nanofluid heat transfer using CVFEM. Neural Computing and Applications. 2016;**27**:1-10. DOI: 10.1007/s00521-016-2740-7

[50] Sheikholeslami M. Influence of Lorentz forces on nanofluid flow in a porous cylinder considering Darcy model. Journal of Molecular Liquids. 2017;**225**:903-912. DOI: 10.1016/j.molliq.2016.11.022

[51] Sheikholeslami M. CVFEM for magnetic nanofluid convective heat transfer in a porous curved enclosure. The European Physical Journal Plus. 2016;**131**:413. DOI: 10.1140/epjp/i2016-16413-y

[52] Sheikholeslami M. Influence of Coulomb forces on Fe_3O_4-H_2O nanofluid thermal improvement. International Journal of Hydrogen Energy. 2017;**42**:821-829. DOI: 10.1016/j.ijhydene.2016.09.185

[53] Kandelousi MS. Effect of spatially variable magnetic field on ferrofluid flow and heat transfer considering constant heat flux boundary condition. The European Physical Journal Plus. 2014;**129**:248. DOI: 10.1140/epjp/i2014-14248-2

[54] Sheikholeslami M. Magnetic field influence on CuO-H_2O nanofluid convective flow in a permeable cavity considering various shapes for nanoparticles. International Journal Of Hydrogen Energy. 2017;**42**:19611-19621. DOI: 10.1016/j.ijhydene.2017.06.121

[55] Sheikholeslami M, Rokni HB. Nanofluid two phase model analysis in existence of induced magnetic field. International Journal of Heat and Mass Transfer. 2017;**107**:288-299. DOI: 10.1016/j.ijheatmasstransfer.2016.10.130

[56] Sheikholeslami M, Sadoughi M. Mesoscopic method for MHD nanofluid flow inside a porous cavity considering various shapes of nanoparticles. International Journal of Heat and Mass Transfer. 2017;**113**:106-114. DOI: 10.1016/j.ijheatmasstransfer.2017.05.054

[57] Sheikholeslami M, Shehzad SA. CVFEM for influence of external magnetic source on Fe_3O_4-H_2O nanofluid behavior in a permeable cavity considering shape effect. International Journal of Heat and Mass Transfer. 2017;**115**:180-191. DOI: 10.1016/j.ijheatmasstransfer.2017.07.045

[58] Sheikholeslami M, Bhatti MM. Active method for nanofluid heat transfer enhancement by means of EHD. International Journal of Heat and Mass Transfer. 2017;**109**:115-122. DOI: 10.1016/j.ijheatmasstransfer.2017.01.115

[59] Randolph T, Fischer G, Kahn J, Kaufman H, Zhurin V, Kozubsky K, Kim V. The mitigation of discharge oscillations in the stationary plasma thruster. In: 30th AIAA/ASME/SAE/ASEE Joint Propulsion Conference; June 27–29, 1994; Indianapolis. 1994. p. AIAA-94-2587

[60] Liqiu W, Liang H, Yongjie D, Daren Y, Chaohai Z. Stabilizing low-frequency oscillation with two-stage filter in Hall thrusters. Review of Scientific Instruments. 2017;**88**(7):073502. DOI: 10.1063/1.4990045

IntechOpen